(2) Nakanishi, F.; Nakanishi, H.; Hasegawa, M. *Nippon Kagaku Kaishi* **1976**, 1575–8.
(3) Birks, J. B., "Photophysics of Aromatic Hydrocarbons"; Wiley: New York, 1970; Chapter 7.
(4) Reiser, A.; Leyshon, L J.; Saunders, D.; Mijovic, M. V.; Bright, A.; Bogie, J. *J. Am. Chem. Soc.* **1972**, *94*, 2414.
(5) Melhuish, W. H. *J. Opt. Soc. Am.* **1952**, *52*, 1256.
(6) Berlman, I. B. "Handbook of Fluorescence Spectra of Aromatic Molecules"; Academic Press: New York, 1965; p 188.
(7) Parker, C. A.; Rees, W. T. *Analyst (London)* **1960**, *85*, 587.
(8) Ghiggino, K. P.; Roberts, A. J.; Phillips, D. *J. Phys. E* **1980**, *13*, 446.
(9) Hackett, P. A.; Phillips, D. *J. Phys. Chem.* **1974**, *78*, 671.
(10) Roberts, A. J.; Phillips, D.; Abdul-Rasoul, F. A. M.; Ledwith, A. *J. Chem. Soc., Faraday Trans. 1*, in press.
(11) Roberts, A. J.; O'Connor, D. V.; Phillips, D. *Ann. N.Y. Acad. Sci.*, in press.
(12) Archer, M. D.; Ferreira, M. I. C.; Porter, G.; Tredwell, C. J. *Nouv. J. Chim.* **1977**, *1*, 9.
(13) Searle, G. F. W.; Barber, J.; Porter, G.; Tredwell, C. J. *Biochem. Biophys. Acta* **1978**, *501*, 246.
(14) Reiser, A.; Egerton, P. L. *Photogr. Sci. Eng.* **1979**, *23*, 144.
(15) Murrell, J. N. "The Theory of the Electronic Spectra of Organic Molecules"; Methuen: London, 1963; Chapter 4.
(16) Stevens, B.; Ban, M. I. *Trans. Faraday Soc.* **1964**, *60*, 1515.
(17) Lamola, A. A. In "Energy Transfer and Organic Photochemistry"; Lamola, A. A., Turro, N. J., Eds.; Interscience: New York, 1969; p 34.
(18) Turro, N. J. "Modern Molecular Photochemistry"; W. A. Benjamin: Menlo Park, Calif., 1978; pp 140.
(19) Williams, J. L. R.; Daly, R. C. *Prog. Polym. Sci.* **1977**, *5*, 61.
(20) Ghiggino, K. P.; Wright, R. D.; Phillips, D. *J. Polym. Sci., Polym. Phys. Ed.* **1978**, *16*, 1499.
(21) Aspler, J. S.; Hoyle, C. E.; Guillet, J. E. *Macromolecules* **1978**, *11*, 925.
(22) Heisel, F.; Laustriat, G. *J. Chim. Phys.* **1969**, *66*, 1881, 1895.
(23) Frank, C. W.; Harrah, L. A. *J. Chem. Phys.* **1974**, *61*, 1526.
(24) Daoud, M.; Cotton, J. P.; Farnoux, B.; Jannink, G.; Sarma, G.; Benoit, H.; Duplessix, R.; Picot, C.; de Gennes, P. G. *Macromolecules* **1975**, *8*, 804.
(25) Nishihara, T.; Kaneko, M. *Makromol. Chem.* **1969**, *124*, 84.
(26) Wolf, C. *Eur. Polym. J.* **1977**, *13*, 739.
(27) Destor, C.; Langevin, D.; Rondelez, R. *J. Polym. Sci., Polym. Lett. Ed.* **1978**, *16*, 229.
(28) de Gennes, P. G. *Macromolecules* **1976**, *9*, 587.
(29) Brochard, F.; de Gennes, P. G. *Macromolecules* **1977**, *10*, 1157.
(30) Pouyet, G.; Francois, J.; Dayantis, J.; Weill, G. *Macromolecules* **1980**, *13*, 176.
(31) Roots, J.; Nystrom, B. *Eur. Polym. J.* **1979**, *15*, 1127.
(32) Reiser, A.; Egerton, P. L. *Macromolecules* **1979**, *12*, 670.

Vibrational Spectra and Disorder–Order Transition of Poly(vinylidene fluoride) Form III

Kohji Tashiro, Masamichi Kobayashi, and Hiroyuki Tadokoro*

Department of Macromolecular Science, Faculty of Science, Osaka University, Toyonaka, Osaka 560, Japan. *Received April 28, 1981*

ABSTRACT: Infrared and Raman spectra of poly(vinylidene fluoride) crystal form III with $T_3GT_3\bar{G}$ molecular conformation have been analyzed by factor group analysis and normal coordinate treatments. Vibrational bands characteristic of some kinds of conformational sequences have been identified: the bands at 299, 776, 811, 1115, and 1134 cm^{-1} for the T_3G sequence, the bands at 1385, 858, and 614 cm^{-1} for the TG sequence, and the bands at 350, 370, 432, 442, 512, 539, 748, 835, 1234, and 1330 cm^{-1} for the TT sequence. Annealing of the form III sample cast from dimethylacetamide solution results in increased intensities of the T_3G and TG infrared and Raman bands and decreased intensities of the trans bands. It also results in a high-temperature shift of the DSC melting point, in the sharpening of low-frequency infrared bands (including lattice modes), and in the intensification of X-ray diffraction spots. These experimental observations have been explained by the following disorder–order structural change induced by the heat-treatment process. The as-cast (unannealed) form III crystal consists of disordered chains containing to some extent long trans sequences within the basic repeat $T_3GT_3\bar{G}$ units (...TTTGTTT$\bar{G}$TTTTTTTTTGTTT$\bar{G}$TT...). Annealing at a temperature close to the melting point induces an interchange between gauche and trans rotational isomers, and the molecular chains become much more ordered with regularly repeating $T_3GT_3\bar{G}$ (...TTTGTTT$\bar{G}$TTTGTTT$\bar{G}$...) units.

It has been reported that poly(vinylidene fluoride) (PVDF) crystallizes into at least four types of crystal forms, namely, forms I, II, III, and polar form II (II_p), depending on the crystallization temperature,[1,2] mechanical stress,[3–7] casting solvent,[4,8,9] electric field,[10–14] and other crystallization conditions. In a previous paper[9] we analyzed the vibrational spectra of crystal forms I, II, and III by normal coordinate treatments and confirmed that form III exists as a crystal phase independent of forms I and II. The infrared and Raman spectra of form III cast from a dimethylacetamide (DMA) solution could be explained approximately in terms of an all-trans conformation molecular model because these spectra of the "as-cast" form III are similar to those of form I over the entire 4000–30-cm^{-1} frequency region (Figure 1). For the high-frequency region of the infrared spectra, Cortili and Zerbi[8] also indicated the similarity of the spectra of form I and form III cast from a dimethyl sulfoxide (Me_2SO) solution. In our previous paper,[9] however, there still remained some problems in interpreting the difference in some parts of the spectra between forms I and III.

Recently, Lando et al.[15] succeeded in obtaining X-ray fiber photographs of uniaxially oriented fiber specimens of crystalline form III that were obtained by stretching the cast film at a temperature immediately below the melting point and proposed that the molecular chain of form III may have one of several possible molecular models, $T_3GT_3\bar{G}$, TGT$\bar{G}$TG$\bar{G}$TG, and so on, but not the planar-zigzag conformation of form I. Banik et al.[16–18] supported this suggestion by potential energy calculations. Bachmann et al.[19] obtained the "crystalline" infrared spectra (as they called it) of form III as a difference between the spectra measured before and after annealing of the as-cast form III by Fourier transform infrared spectroscopy. They stated that the weak infrared bands appearing in the spectra of crystalline form III correspond to the gauche bands of form II (molecular conformation TG$\bar{G}$) and supported the proposal made by Lando et al.,[15] although

0024-9297/81/2214-1757$01.25/0

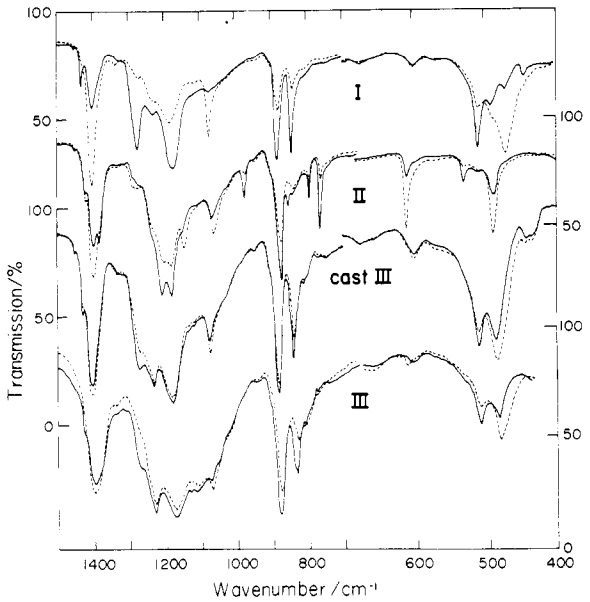

Figure 1. Polarized infrared spectra of PVDF crystal forms I, II, III (cast from DMA solution and rolled slightly), and crystalline III. The solid and broken lines represent, respectively, the spectra measured with an incident electric vector perpendicular and parallel to the stretched axes.

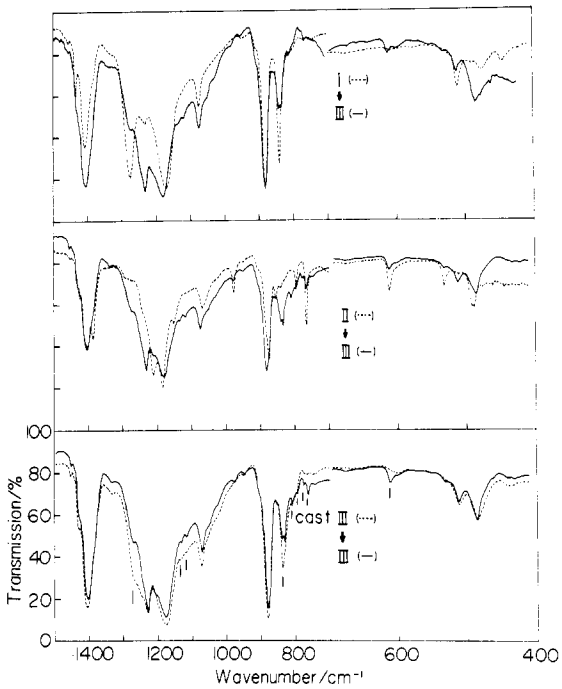

Figure 2. Spectral changes corresponding to the transformation from crystal forms I, II, and as-cast III to annealed form III induced by heat treatment at a temperature immediately below the melting points. The broken and solid lines represent the unpolarized infrared spectra measured before and after heat treatment, respectively.

they could not determine finally which model was the most reasonable for crystalline form III. Lando et al.[20] reported recently the molecular and crystal structures of crystalline form III by X-ray analysis (the number of observed X-ray reflections was 21): an orthorhombic cell of a = 4.97 Å, b = 9.66 Å, and c (fiber axis) = 9.18 Å and molecular conformation $T_3GT_3\bar{G}$. Quite independently, Takahashi and Tadokoro[21] succeeded in obtaining a highly oriented crystalline sample of form III by annealing a form II sample having streaky X-ray reflections for a long time. They analyzed the molecular and crystal structures using 47 independent X-ray reflections and reported a monoclinic cell of a = 4.96 Å, b = 9.58 Å, c (fiber axis) = 9.23 Å, and β = 92.9° and molecular conformation $T_3GT_3\bar{G}$. This monoclinic unit cell is supported by Lovinger's[22] electron diffraction photographs.

Thus the molecular conformation of form III can be said to be confirmed by X-ray structure analysis. But we must still clarify some problems in the interpretation of the vibrational spectra: The infrared and Raman spectra of the as-cast form III are similar to those of form I, whereas those of the highly annealed form III have some infrared bands characteristic of form II. These problems will be discussed in this paper.

Experimental Section

Samples. Commercial PVDF samples were used: Kynar 201 (Pennwalt Chemical Co., Ltd., mp ~173 °C) and KF 1000 (Kureha Chemical Industry Co., Ltd., mp ~185 °C). Films of forms I, II, and III were prepared as follows:[9]

Form I. An unoriented sample was prepared by casting slowly from hexamethylphosphoric triamide solution at room temperature. A uniaxially oriented sample was prepared by stretching an unoriented form II sample at room temperature.

Form II. An unoriented sample was prepared by casting from acetone solution at about 50 °C or by slowly cooling the melt to room temperature. An oriented sample was prepared by stretching the unoriented sample at about 150 °C.

Form III. An unoriented sample was slowly cast from DMA solution on a glass plate at about 65 °C or cooled slowly from the molten state (the sample prepared by the latter method contained some form II and the content of form III varied from sample to sample depending on the cooling rate). An oriented sample of form III was prepared as follows. (a) An unoriented sample of form III cast from DMA solution was rolled at room temperature (elongation ratio less than 200–300% of the original length). (b) An oriented film of form II containing a small amount of form III was annealed at a temperature about 10 °C below the melting point for about 100 h.[1,2] The ease of transformation from form II to form III on annealing was governed by the initial content of form III; i.e., the higher content of form III was obtained by annealing the form II sample containing the higher initial amount of form III. (c) Unoriented films of form III were stretched immediately below the melting point.[15] It was difficult to obtain oriented form III by hand or machine extension because form III transforms so easily to form I under mechanical stress. The following method was therefore adopted. Both ends of a slender sample film were sandwiched between two pairs of small magnets. The sample was then hung in a test tube filled with silicone oil. This test tube was put into an oil bath heated to about 180 °C (for KF polymer). After a few minutes the temperature in the tube rose close to that of the bath, and at that point the sample weighted by the magnets was stretched spontaneously with the help of gravitational force. At about 300–400% extension, the test tube was removed from the bath and cooled to room temperature. The drawn sample was washed with petroleum ether and dried.

Measurements. Infrared spectra were measured with Japan Spectroscopic Co. DS-402G and A-III infrared spectrophotometers (4000–400 cm^{-1}) and a Hitachi FIS-3 far-infrared spectrophotometer (400–30 cm^{-1}). Raman spectra were obtained with a Japan Spectroscopic Co. R-500 double-monochromator instrument. The 5145-Å line from an argon ion laser was used as an excitation light source. Wide-angle X-ray diffraction patterns were obtained by using nickel-filtered Cu Kα radiation with a cylindrical camera and also with a diffractometer. Melting points were measured with Rigaku-Denki differential scanning calorimeter. The heating rate was 10 °C/min.

Results and Discussion

Infrared and Raman Spectra of Crystalline Form III. Prest and Luca[1] and Osaki and Ishida[2] reported that the infrared spectra of form III could be obtained by annealing form II for a substantial time immediately below

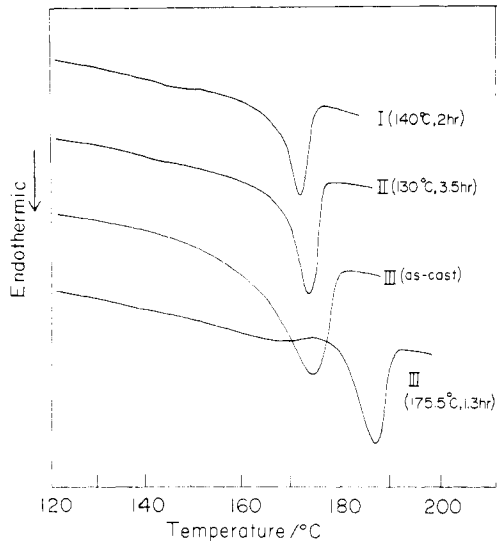

Figure 3. DSC curves for PVDF forms I, II, as-cast III, and annealed III. The heating rate was 10 °C/min.

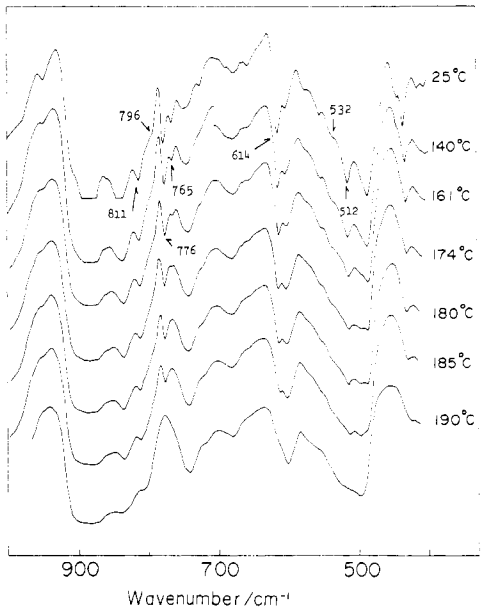

Figure 4. Temperature dependence of infrared spectra for annealed PVDF form III sample.

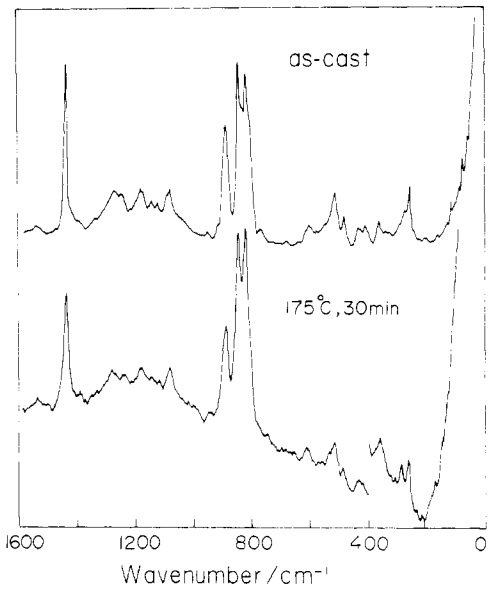

Figure 5. Annealing effect on unpolarized Raman spectra of PVDF form III.

the melting point. As shown in Figure 2, we have found that the infrared spectra of crystalline form III can be obtained from the crystal forms of both I and II and also from the as-cast form III by heat treatment at 155–160 °C (for Kynar samples). It is observed in Figure 2 not only that the infrared spectra of forms I, II, and III are different from each other but also that the spectra of the as-cast form III are appreciably different from those of crystalline form III. The infrared spectra of as-cast form III have intense bands at 1275 and 840 cm^{-1} in addition to the bands characteristic of form III (1134, 1115, 811, and 776 cm^{-1} and so on), while the spectra of annealed form III have bands corresponding to those of form II (614 cm^{-1} and so on). At the same time the 1275- and 840-cm^{-1} bands decrease remarkably in intensity. Bachmann et al.[19] recognized *all* of the bands appearing in the infrared spectra of annealed form III as characteristic of crystalline form III, and they concluded that form III has a molecular conformation consisting of both trans and gauche bonds. But from our observations that the lattice vibrational band characteristic of the form II crystal phase is observed in the far-infrared spectrum of the annealed form III film and that the relative intensities of several bands corresponding to form II vary from sample to sample depending on the preparation conditions, there is still a possibility that some of the bands in the infrared spectra of annealed form III originate from a contamination of form II crystalline phase in the sample. Therefore it is necessary to distinguish the bands truly characteristic of crystalline form III from those of form II. As shown in Figure 3, the melting points of form II and crystalline form III differ by about 10 °C (the difference in melting points between the as-cast sample and the annealed sample of form III will be discussed in a later section). Thus, when the infrared spectra are measured at high temperature around the melting point, the infrared bands of crystalline form III can be expected to remain observable even at a temperature where the form II bands disappear due to the melting of form II crystals.[2] Figure 4 shows the temperature dependence of the infrared spectra for annealed form III sample in the temperature range from room temperature to 190 °C (for KF polymer). The bands at 796, 765, and 532 cm^{-1}, for example, disappear at 170 °C (melting point of form II), while the bands at 811, 776, and 512 cm^{-1}, still observable at this temperature, disappear at a higher temperature, about 187 °C (melting point of form III). (The band at 539 cm^{-1}, still observable at 180 °C as a shoulder, is characteristic of form III and not of form II (532 cm^{-1}). Refer to Table II.) Thus the former bands should be considered to be due to form II crystal. The band at 614 cm^{-1} is common to forms II and III and does not disappear even at the temperature where the form II bands are not detected. Therefore the 614-cm^{-1} band, characteristic of the gauche conformation, should be assigned to the crystalline forms of both II and III. The existence of the gauche band thus confirmed cannot be explained in terms of an all-trans conformation as predicted in the previous paper[9] for the model of as-cast form III. The observed total number of crystalline form III bands is about 50 (from 4000 to 30 cm^{-1}), too large to support the all-trans model, as Bachmann et al. already pointed out.[19] The circumstances stated here are also observed in the case of the Raman spectra. For example, the 811-cm^{-1} band greatly increases its intensity upon annealing, as shown in Figure 5, and should be assigned to the crystalline band characteristic of form III. This

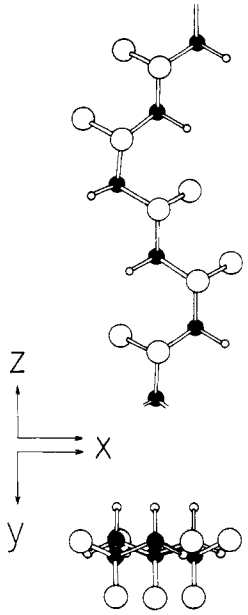

Figure 6. Molecular conformation of PVDF form III.[20,21]

Table I
Factor Group Analysis for a $T_3GT_3\bar{G}$ Conformation of PVDF Form III

C_s	E	σ_g	IR[a]	Raman[b]	n[c]
A′	1	1	μ_z, μ_y	$\alpha_{xx}, \alpha_{yy}, \alpha_{zz}, \alpha_{yz}$	34
A″	1	−1	μ_x	α_{zx}, α_{xy}	34

[a] μ_i denotes a transition moment vector. The Cartesian coordinate axes are defined in Figure 6. [b] α_{ij} denotes a polarizability tensor component. [c] n denotes the number of internal normal modes.

intense band does not appear in the Raman spectra of form I crystal and also cannot be explained in terms of an all-trans conformation. In the following section we will try to analyze the vibrational spectra of crystalline form III thus clarified by using the $T_3GT_3\bar{G}$ conformational model indicated by X-ray.

Normal Coordinate Treatments of PVDF Form III Chain. As shown in Figure 6, the chain conformation of crystalline form III ($T_3GT_3\bar{G}$) has a glide-plane symmetry along the chain direction,[20,21] the factor group of which is isomorphous with the point group C_s. In Table I is shown the result of the factor group analysis of a single chain of $T_3GT_3\bar{G}$, where the coordinate axes are defined as the z axis parallel to the chain axis, the x axis normal to the glide plane, and the y axis normal to the z axis in the glide plane. The factor group analysis predicts 34 bands for the A′ symmetry species and the 34 for the A″ species; i.e., a total of 68 vibrational bands is expected to appear in both the infrared and Raman spectra. Distinction between the A′ and A″ species can be made from polarization measurements of the spectra as shown in Table I. Only the A′ bands show the parallel infrared dichroism and the Raman polarized component of (zz) polarization. In Figures 1, 7, and 8 are shown, respectively, the polarized infrared, far-infrared, and Raman spectra for the uniaxially oriented crystalline form III samples. The observed results are listed in Table II.

Normal coordinate treatments have been carried out for an isolated chain of $T_3GT_3\bar{G}$ conformation based on Wilson's GF matrix method.[23] The molecular parameters utilized are as follows: bond lengths, C–C = 1.54, C–F = 1.34, C–H = 1.09 Å; bond angles, CCC = 115.0, HCH = 112.0, FCF = 109.9, CCH = 107.5, CCF = 108.0°; internal rotation angles of the skeletal sequences, trans (T) 180.0° and gauche (G) 60.0°. Valence force field (VFF) type force constants are adopted for the intramolecular forces, the values of which are determined by least-squares calculation of the observed vibrational frequencies using the initial values reported in the previous paper.[9] The results are listed in Table III. The calculated wavenumbers and band assignments are shown in Table II in comparison with the observed wavenumbers, where the notations "t" and "g" of the potential energy distributions (PED) indicate that the vibrational energy concentrates on the atomic group of the trans (TT) and gauche (TG) sequences, respectively; for example, if the symmetric stretching mode of the CF_2 group in the $-CH_{2\bar{T}}CF_{2\bar{G}}CH_2-$ sequence has a PED of

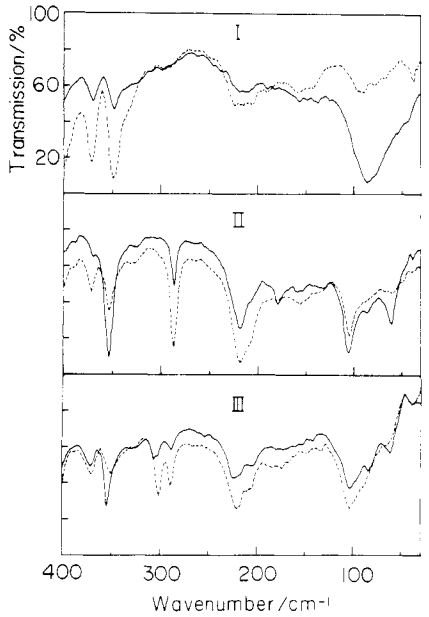

Figure 7. Polarized far-infrared spectra of PVDF forms I, II, and III. The solid and broken lines represent the spectra measured with an incident electric vector perpendicular and parallel to the stretched axes, respectively. In the sample of form III are contained some amounts of form II crystal.

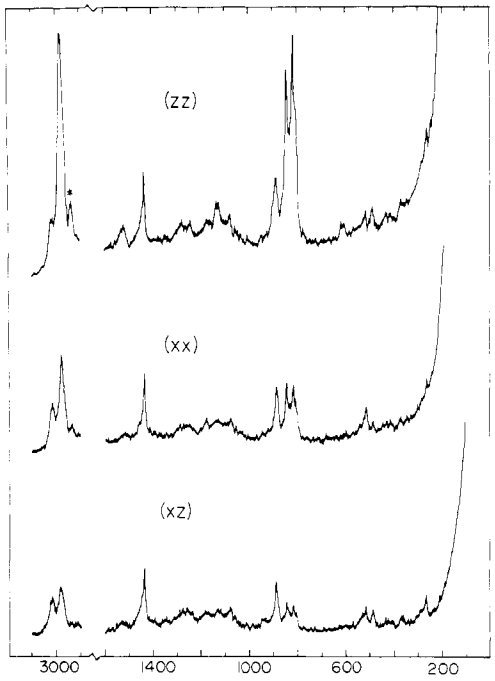

Figure 8. Polarized Raman spectra of uniaxially oriented PVDF form III. The z axis is parallel to the stretching direction and the x and y axes are normal to the z axis.

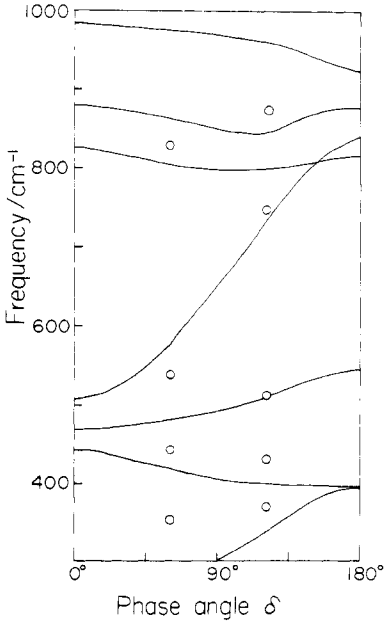

Figure 9. Trans bands of PVDF form III and dispersion curves calculated for the all-trans conformation of form I.[9] The phase angle δ, $\pi/3$ or $2\pi/3$, is estimated from the calculated L vector for each mode.

50%, it is represented as $\nu_s(CF_2)(50g)$. In the table only the modes having a PED contribution larger than 15% are listed. From the table it can be observed that some kinds of vibrational waves localize on trans or gauche sequences (the PED concentrates on the t or g part) and some waves cover the whole $T_3GT_3\bar{G}$ sequence (the PED is distributed over both the t and g parts). Since the molecular structure of form III has a TTT sequence, the trans bands localized at such a T_3 sequence may be expected to correspond approximately to the points where $\delta = k\pi/(m+1) = \pi/3$ and $2\pi/3$ ($m = 2$ and $k = 1$ and 2) on the frequency dispersion curves of the all-trans form I chain as predicted from the simple coupled oscillator model,[24] where δ is a phase difference between the neighboring CH_2CF_2 monomer units. In fact, as shown in Figure 9, the bands having nearly exclusively the "trans" PED, for example, 350, 370, 432, 512, 539, 835, 1234, and 1330 cm^{-1}, fit fairly well on the dispersion curves calculated for the all-trans chain conformation of form I,[9] although they may deviate more or less from the exact positions of the curves because of some degree of vibrational coupling between the trans and gauche parts. The band at 614 cm^{-1}, corresponding to the form II band, has a PED of $\delta(CF_2)(58g)$ and is the so-called gauche band. Such characteristic bands of the gauche part can be observed at 1385 and 858 cm^{-1}. The 811-cm^{-1} band has a very weak infrared intensity but the strongest Raman intensity, which is increased by heat treatment as shown in Figure 5. It should thus be assigned to the normal vibration characteristic of crystalline form III. The normal mode calculation also supports this consideration: this band is assigned to the rocking mode of the CH_2 group with a calculated frequency 792 cm^{-1} and the PED to both the t and g parts; in other words, the vibrational wave extends over the whole $T_3GT_3\bar{G}$ unit. Such characteristic bands of form III are also observed at 299, 776, 1115, and 1134 cm^{-1} and so on.

These band assignments to trans and gauche sequences can also be confirmed reasonably from comparison of the infrared spectra of the three crystalline forms shown in Figure 2. The band at 1275 cm^{-1}, for example, which is intense in the spectra of form I and very weak in those of

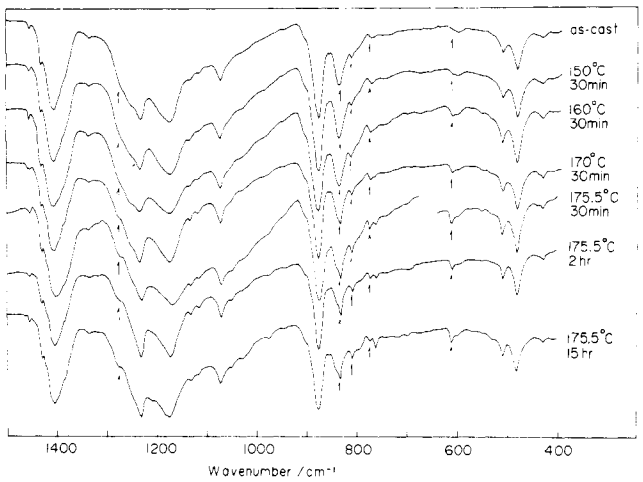

Figure 10. Infrared spectral changes induced by heat treatment of as-cast PVDF form III.

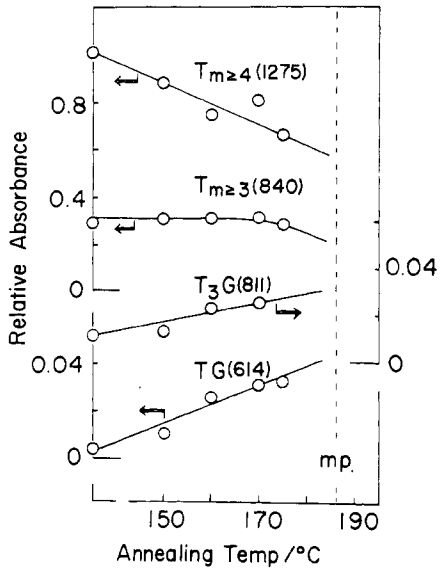

Figure 11. Annealing effect on the relative absorbances for as-cast PVDF form III (refer to Figure 10).

forms II and III, is considered to appear when the chain has a long trans sequence. The band at 839 cm^{-1}, present in the spectra of forms I and III but not in the spectra of form II, may originate from conformations having trans sequences longer than TT. The band at 614 cm^{-1} is assigned to gauche conformations because it appears strongly in the form II spectra and weakly in the form III spectra and disappears in the form I spectra as stated already. Similarly, as shown in Figure 7, the far-infrared band at 299 cm^{-1} (parallel band) appears only in the form III spectra and has a PED to both of the trans and gauche parts (Table II). Thus it is characteristic of the T_3G conformation as already pointed out. In the next section we discuss the changes in the intensities of these bands induced by heat treatment of the as-cast (unannealed) form III samples.

Disorder-to-Order Transition in PVDF Form III. Figure 10 shows the annealing-temperature dependence of the infrared spectra of the as-cast form III film. As the annealing temperature rises close to the melting point, the trans bands are reduced and the gauche bands increase gradually in intensity. In Figure 11 is shown the dependence of the relative absorbances of these bands on the annealing temperature, where an individual component of the bands has been separated from the others by assuming

Table II
Band Assignments for Crystalline Form III

obsd[a]	calcd[a]	rel intens[b]	PED,[c] %
		A′ (IR, ∥, ⊥; Raman, α_{xx}, α_{yy}, α_{zz}, α_{yz})	
3032	3027	vw	$\nu_{as}(CH_2)(74g - 26t)$
3022	3026	vvw	$\nu_{as}(CH_2)(74t + 26g)$
2990	2987	vw	$\nu_s(CH_2)(54g + 45t)$
2985	2987	vvw	$\nu_s(CH_2)(54t + 45g)$
1400	1404	vs	$\delta(CH_2)(55t + 16g)$
1385	1380	vs	$\delta(CH_2)(69g)$
1365	1370	sh	$\delta(CH_2)(23t) - w(CH_2)(42g)$
1320	1320	vvw	$w(CH_2)(67t)$
1250	1254	sh	$\nu_{as}(CF_2)(44g) + w(CH_2)(16g)$
1234	1245	vs	$\nu_{as}(CF_2)(65t) - r(CF_2)(19t)$
1190?	1188	sh	$\nu_s(CF_2)(31g)$
1175	1169	vs	$\nu_s(CF_2)(36t)$
	1095		$\nu(CC)(23t - 20g) + w(CF_2)(18g)$
1075	1062	m	$\nu(CC)(23t - 19t - 15g) + w(CF_2)(19t)$
964	964	sh	$t(CH_2)(54t - 38g)$
	932		$t(CH_2)(41g + 32t)$
874	879	vs	$\nu(CC)(12g + 16t - 22t)$
858	862	vw	$\nu_s(CF_2)(54g)$
835	839	m	$\nu_s(CF_2)(49t) + \nu(CC)(13t)$
811	792	w	$r(CH_2)(35g - 18t)$
776	764	w	$r(CH_2)(47t + 26g)$
614	561	w	$\delta(CF_2)(58g)$
539	548	sh	$\delta(CF_2)(36t)$
484	490	s	$\delta(CF_2)(46t) - w(CF_2)(16g)$
442	432	w	$r(CF_2)(48t) - r(CH_2)(21t)$
	399		$r(CF_2)(36g + 18t)$
370	377	m	$t(CF_2)(30t)$
299	301	m	$\delta(CF_2)(29g) + w(CF_2)(17t) - t(CF_2)(11t)$
286	273	w	$t(CF_2)(56g - 35t)$
172	168	w	$\delta(CCC)(30t + 19t)$
130	129	w	$\delta(CCC)(33t - 13g - 20t)$
98[d]	84	s	$\delta(CCC)(23g + 13t) + \tau(CCCC)(16t)$
84[d]	45	sh	$\tau(CCCC)(37g - 25t)$
	32		$\tau(CCCC)(14t + 55t - 15t + 12g)$
		A″ (IR, ⊥; Raman, α_{xz}, α_{xy})	
3032	3027	vw	$\nu_{as}(CH_2)(99g)$
3022	3027	vvw	$\nu_{as}(CH_2)(99t)$
2990	2988	vw	$\nu_s(CH_2)(48g - 51t)$
2985	2986	vvw	$\nu_s(CH_2)(48g + 51t)$
1427	1424	w	$\delta(CH_2)(40t) + w(CH_2)(17g)$
1385	1385	vs	$\delta(CH_2)(69g) + w(CH_2)(16g)$
1365	1363	sh	$\delta(CH_2)(16g + 39t) - w(CH_2)(22g)$
1330	1325	vvw	$w(CH_2)(59t)$
1274	1246	w (sh)	$\nu_{as}(CF_2)(34t - 21g)$
	1243		$\nu_{as}(CF_2)(32t + 21g)$
1205	1198	w	$\nu_s(CF_2)(22t - 13g)$
1134	1142	w	$\nu(CC)(20g - 20t) - w(CF_2)(17g)$
1115	1119	w	$\nu_s(CF_2)(18t + 35g)$
1052	1065	sh	$\nu(CC)(20t + 10g - 12t + 19t) + w(CF_2)(17t)$
	950		$t(CH_2)(70t + 17g)$
	945		$t(CH_2)(63g - 15t)$
878	872	sh	$\nu_s(CF_2)(59t)$
842	839	m	$\nu_s(CF_2)(25g) + \nu(CC)(25t)$
791	797	vw	$r(CH_2)(45g)$
748	775	w	$r(CH_2)(65t)$
723	737	vw	$\nu(CC)(20g) + w(CF_2)(14t)$
656	652	vw	$w(CF_2)(28g) + \nu(CC)(26t)$
512	534	m	$\delta(CF_2)(48t)$
500?	499	sh	$\delta(CF_2)(56g - 17t)$
432	430	w	$r(CF_2)(55t)$
404	417	vw	$r(CF_2)(39g)$
350	346	m	$t(CF_2)(35t)$
304	303	w	$t(CF_2)(70g)$
267?	276	vvw	$t(CF_2)(35t) - \delta(CCC)(16g)$
172	164	w	$\delta(CCC)(21g + 35t) - w(CF_2)(22t)$
	79		$\tau(CCCC)(19g - 13t)$
	63		$\tau(CCCC)(11g + 27t - 24t)$
	32		$\tau(CCCC)(11g - 28t - 14t + 40t)$

[a] Wavenumber (cm^{-1}). [b] Rel intens = relative intensity: vs, very strong; s, strong; m, medium; w, weak; vw, very weak; vvw, very very weak; sh, shoulder. The relative intensities in the frequency region lower than 400 cm^{-1} are not related with those of the higher frequency region. [c] PED: potential energy distribution. The notations "t" and "g" are explained in the text. Symmetry coordinates: ν_s, symmetric stretching; ν_{as}, antisymmetric stretching; δ, bending; w, wagging; t, twisting; r, rocking; τ, torsional mode. The sign + or − denotes the phase relation among the symmetry coordinates. [d] These bands should contain some contributions from the lattice vibrational modes and so the assignments in terms of the intramolecular symmetry coordinates may be considered to be only tentative.

Table III
Intramolecular Valence Force Constants for Poly(vinylidene fluoride) Form III

no.	force constant	coordinates involved	common atoms	values[a]
1	K_d	CH		4.923
2	K_R	CC		4.257
3	F_{Rl}	CC, CF	C	0.149
4	F_R	CC, CC	C	0.497
5	F_{Rr}	CC, CCH	CC	0.238
6	F_{Rw}	CC, CCC	CC	0.240
7	$F_{R\phi}$	CC, CCF	CC	0.464
8	F_d	CH, CH	C	0.073
9	K_l	CF		6.357
10	F_{ll}	CF, CF	C	1.111
11	$F_{l\zeta}$	CF, CFF	CF	1.431
12	H_r	CCH		0.581
13	F_r	CCH, CCH	CC	0.115
14	F_r'	CCH, CCH	CH	0.041
15	H_δ	CHH		0.451
16	H_w	CCC		1.357
17	f_w^t	CCC, CCC (t)	CC	−0.210
18	H_ϕ	CCF		1.365
19	H_ζ	CFF		1.306
20	T	CCCC		0.059
21	$F_{l\phi}$	CF, CCF	CF	0.546
22	F_ϕ	CCF, CCF	CC	0.230
23	F_ϕ'	CCF, CCF	CF	0.200
24	f_w^g	CCC, CCC (g)	CC	−0.625
25	f_{wr}^g	CCC, CCH (g)	CC	0.180
26	f_{wr}^t	CCC, CCH (t)	CC	0.064
27	$f_{w\phi}^g$	CCC, CCF (g)	CC	−0.170
28	$f_{w\phi}^t$	CCC, CCF (t)	CC	−0.151
29	$f_{r\phi}^t$	CCH, CCF (t)	CC	0.075
30	$f_{r\phi}^g$	CCH, CCF (g)	CC	0.027

[a] The stretch constants have units of mdyn/A, the stretch-bend interaction constants have units of mdyn/rad, and the bending constants have units of mdyn Å/rad².

a Lorentzian function, the integrated intensity being adopted as the absorbance. Since the absorbance of the 877-cm^{-1} band is almost proportional to the thickness of the sample film and does not depend on the state of the sample, it is used as an internal standard. As understood from the figure, the bands of long trans sequences (1275 and 840 cm^{-1}) decrease in intensity and the band intensities of the gauche (614 cm^{-1}) and T_3G sequences (811 and 776 cm^{-1} and so on) increase steadily.

In addition to these heat treatment induced spectral changes of the as-cast form III, the DSC curves, the far-infrared low-frequency bands, and the X-ray diffraction curves change as shown in Figures 3, 7, and 12. In Figure 3 the melting point of form III crystal shifts to higher temperature by about 10 °C, from 174 to 186 °C, when the as-cast sample is annealed. At the same time the sharpness of the endothermic peak increases appreciably. In the far-infrared spectra of Figure 7, not only the T_3G band (299 cm^{-1}) intrinsic of crystalline form III but also the low-frequency band at about 90 cm^{-1}, which may be a coupling vibration of the skeletal torsional mode and the librational lattice mode, increase in intensity as heat treatment proceeds. In Figure 12 the annealing process intensifies and sharpens the X-ray diffraction patterns of the unoriented form III sample.

On the basis of all of these experimental results we can specify the difference in structural feature between as-cast form III and crystalline form III as follows. As-cast form III takes a more or less disordered molecular conformation containing a fairly long trans unit in the basic $T_3GT_3\bar{G}$ sequence. The low degree of the order in the chain packing of the crystal lattice, originating from such a disordered chain structure, is reflected in the broad melting behavior at a comparatively low temperature, in the broadness of

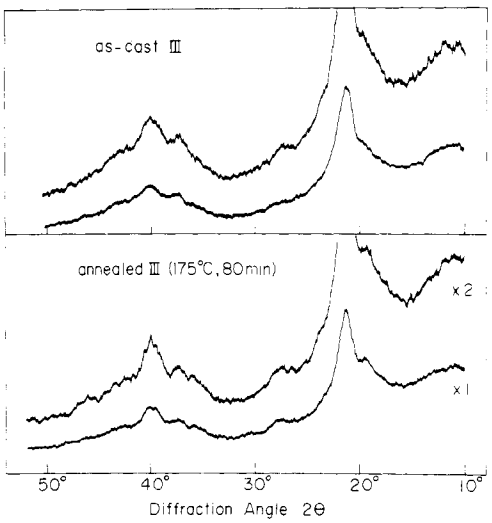

Figure 12. Annealing effect on the X-ray diffraction curves of PVDF form III.

the low-frequency infrared band including a lattice vibrational mode, and in the broadness of the X-ray diffraction patterns. The heat treatment of as-cast form III results in the interchange between the trans and gauche isomers of the skeletal linkages, as revealed by the infrared and Raman spectral measurements, and the molecular chain becomes more regular with a $T_3GT_3\bar{G}$ repeat unit; i.e.

$$\ldots\ldots TTT\bar{G}TTTGTTTTTTT\bar{G}TTTG\ldots\ldots$$
$$\downarrow$$
$$\ldots\ldots TTT\bar{G}TTTGTTT\bar{G}TTTGTTT\bar{G}\ldots\ldots$$

As a result of such a disorder-to-order transition in the molecular conformation, the regularity of the chain lattice increases, as reflected in the high-temperature shift and sharpening of the DSC melting curve, in the sharpening of the vibrational bands, and in the sharpening of the X-ray diffraction pattern. In Figure 10 is also shown the annealing-time dependence of the infrared spectra of form III at 175.5 °C (for KF polymer). As the annealing time increases, the gauche bands characteristic of "form II" (765 cm^{-1} etc.) increase in relative intensities though not so greatly. The statistical balance between the trans and gauche isomers varies with the annealing time and some portions of the $TG\bar{T}\bar{G}$ conformer might be produced in the chain of $T_3GT_3\bar{G}$ sequence. Such an interchange of trans and gauche conformers at high temperature has been already pointed out by Takahashi and Tadokoro[21,25] in explaining the generation of kink bands within form II crystallites and the formation of crystalline form III from form II crystal.

In conclusion, we now give definite answers for the questions mentioned in the introduction. (i) Why are the vibrational spectra of the as-cast (unannealed) form III film so similar to those of form I, having an all-trans conformation? It is because the as-cast form III sample contains a high proportion of long trans sequences as a kind of defect within the basic $T_3GT_3\bar{G}$ conformation and therefore the intense infrared bands characteristic of the long trans sequences are prominent compared with the originally weak and broad bands characteristic of TG and T_3G sequences. (ii) Why are the spectra of the annealed form III sample so different from those of as-cast form III? It is because the heat treatment at a temperature close to the melting point induces interchange between trans and gauche rotational isomers in the disordered molecular

chain of the as-cast form III sample and so the chain becomes much more ordered, resulting in the disappearance of the long trans bands and the appearance of the gauche bands.

Acknowledgment. We are grateful to Kureha Chemical Industry Co., Ltd., for supplying samples of PVDF.

References and Notes

(1) Prest, W. M.; Luca, D. J. *J. Appl. Phys.* **1978**, *49*, 5042.
(2) Osaki, S.; Ishida, Y. *J. Polym. Sci., Polym. Phys. Ed.* **1975**, *13*, 1071.
(3) Hasegawa, R.; Kobayashi, M.; Tadokoro, H. *Polym. J.* **1972**, *3*, 591.
(4) Hasegawa, R.; Takahashi, Y.; Chatani, Y.; Tadokoro, H. *Polym. J.* **1972**, *3*, 600.
(5) Doll, W. W.; Lando, J. B. *J. Macromol. Sci., Phys.* **1970**, *B4*, 889.
(6) Matsushige, K.; Takemura, T. *J. Polym. Sci., Polym. Phys. Ed.* **1978**, *16*, 921.
(7) Scheinbeim, J.; Nakafuku, C.; Newman, B. A.; Pae, K. D. *J. Appl. Phys.* **1979**, *50*, 4399.
(8) Cortili, G.; Zerbi, G. *Spectrochim. Acta, Part A* **1967**, *23a*, 2216.
(9) Kobayashi, M.; Tashiro, K.; Tadokoro, H. *Macromolecules* **1975**, *8*, 158.
(10) Southgate, P. D. *Appl. Phys. Lett.* **1976**, *28*, 250.
(11) DasGupta, D. K.; Doughty, K. *J. Appl. Phys.* **1978**, *49*, 4601.
(12) Davis, G. T.; McKinney, J. E.; Broadhurst, M. G.; Roth, S. C. *J. Appl. Phys.* **1978**, *49*, 4998.
(13) Davies, G. R.; Singh, H. *Polymer* **1979**, *20*, 772.
(14) Servet, B.; Rault, J. *J. Phys. (Paris)* **1979**, *40*, 1145.
(15) Weinhold, S.; Litt, M. H.; Lando, J. B. *J. Polym. Sci., Polym. Lett. Ed.* **1979**, *17*, 585.
(16) Tripathy, S. K.; Potensone, R., Jr.; Hopfinger, A. J.; Banik, N. C.; Taylor, P. L. *Macromolecules* **1979**, *12*, 656.
(17) Banik, N. C.; Taylor, P. L.; Tripathy, S. K.; Hopfinger, A. J. *Macromolecules* **1979**, *12*, 1015.
(18) Banik, N. C.; Boyle, F. P.; Sluckin, T. J.; Taylor, P. L. *J. Chem. Phys.* **1980**, *72*, 3191.
(19) Bachmann, M. A.; Gordon, W. L.; Koenig, J. L.; Lando, J. B. *J. Appl. Phys.* **1979**, *50*, 6106.
(20) Weinhold, S.; Litt, M. H.; Lando, J. B. *Macromolecules* **1980**, *13*, 1178.
(21) Takahashi, Y.; Tadokoro, H. *Macromolecules* **1980**, *13*, 1317.
(22) Lovinger, A. J. *Macromolecules* **1981**, *14*, 322.
(23) Tadokoro, H. "Structure of Crystalline Polymers"; Wiley-Interscience: New York, 1979.
(24) Zbinden, R. "Infrared Spectroscopy of High Polymers"; Academic Press: New York, 1967.
(25) Takahashi, Y.; Tadokoro, H. *Macromolecules* **1980**, *13*, 1316, 1317. Takahashi, Y.; Tadokoro, H.; Odajima, A. *Ibid.* **1980**, *13*, 1318.

Monomer Sequence Distributions in Four-Component Polyesters As Determined by ^{13}C and ^{1}H NMR

G. A. Russell,* P. M. Henrichs,* J. M. Hewitt, H. R. Grashof, and M. A. Sandhu†

Research Laboratories, Eastman Kodak Company, Rochester, New York 14650.
Received April 27, 1981

ABSTRACT: Four-component polyesters derived from ethylene glycol, 1,4-butanediol, azelaic acid, and terephthalic acid have been characterized by ^{13}C and ^{1}H NMR at 63 kG. Derived statistical parameters permit comparison of monomer sequence distributions in multicomponent systems and have been applied to the four-component polyester system. Sequence-dependent chemical shift information has been used to determine these parameters in various samples of the four-component polyester. Melt polycondensation gives polymers having random sequence distributions, whereas sequential addition of diacid chlorides to diols in solution gives polymers in which the diacid residues are arranged in long blocked sequences with the diol groups interspersed randomly within. Alternate addition of the diacid chlorides in several steps in solution leads to a slightly nonrandom polymer with an unequal distribution of the diols between the diacid residues.

Polyesters are used in a number of important materials, including fibers, film supports, injection molding resins, adhesives and adhesive primers, transparency supports, photoresists, and a variety of specialty products. Early commercial polyesters were formed by the condensation of a single type of diol and a single type of diacid or were formed from an ω-hydroxy acid.[1] More recently, two or more types of diacid and/or diol have frequently been incorporated into a given polyester to optimize such properties as the glass transition temperature (T_g), melting point (T_m), crystallizability, solubility, modulus, and tensile strength. As a result, methods which can be used to determine monomer composition and monomer sequence distribution in such materials are important.

Alkaline hydrolysis coupled with gas chromatography[2] or liquid chromatography[3] can be used to determine overall monomer compositions in copolyesters, but it reveals nothing about the monomer sequence distribution. Nuclear magnetic resonance (NMR) is an important tool for characterizing copolyesters because it can, in favorable cases, yield information about overall composition and monomer sequence distribution simultaneously. NMR has been used to study various three-component polyester systems[4,5] and has recently been applied to four-component systems.[6]

We describe here the use of a combination of ^{13}C and ^{1}H NMR to determine the composition and sequence distribution in a four-component copolyester composed of terephthalic (T) and azelaic (A) acid residues with ethylene glycol (E) and butanediol (B). The structures of the monomer units are shown in Figure 1. We have derived a set of statistical parameters which can be used to characterize monomer sequence distributions in four-component polyesters.

Experimental Section

Most of the polymers used in this study were produced by two-stage melt polycondensation of the appropriate diols with the dimethyl esters of the appropriate diacids. The monomers used were commercial materials and were used without further purification. The polymers were transesterified in the melt under nitrogen, and then vacuum was applied to distill off methanol

†Present address: Research Laboratories, Tennessee Eastman Co., Kingsport, Tenn. 37662.

0024-9297/81/2214-1764$01.25/0